LOGO IEEE ELECTRON DEVICE LETTERS, VOL. XX, NO. XX, XXXX 2021

8-Fold Helically Corrugated Interaction Region for High Power Gyroresonant THz Sources

Craig R. Donaldson, Liang Zhang, Michael Harris, Matthew J. Beardsley, Peter G. Huggard, Colin G. Whyte, Adrian W. Cross, and Wenlong He

***Abstract*— A manufacturing study of a 0.372 THz 8-fold (8F) helically corrugated interaction region (HCIR) and measurement of its wave dispersion characteristics are reported. This demonstrates the structure's suitability as the electron beam / electromagnetic wave interaction region in a high power frequency tunable Gyroresonant THz source. The 8F HCIR has an eigenmode, which is ideal for broadband tuning, created by the coupling of the TE_{61} and TE_{23} modes. Maximum power handling of 14 times larger than a 3-fold HCIR at the same frequency is calculated. A TE_{11} to TE_{61} 7-fold (7F) helically corrugated waveguide (HCW) mode converter, needed to measure the wave dispersion of the 8F HCIR, was designed and constructed. Negative aluminium mandrels of the 7F HCW mode converter and 8F HCIR were manufactured. Copper structures were constructed through electroforming. The measured wave dispersion of the 0.372 THz 8F HCIR agreed well with simulated dispersion characteristics.**

***Index Terms*— helically corrugated waveguide; precise manufacture; THz sources**

I. Introduction

THZ power sources are in great demand. Many applications and technologies can be enhanced by operating in the 0.3 THz to 1 THz frequency range at high powers and with wide bandwidths such as in high resolution radar [1], electron paramagnetic resonance (EPR) and dynamic nuclear polarisation enhanced nuclear magnetic resonance (DNP-NMR) spectroscopy [2], telecommunications [3] and so on. Gyro-devices [4] are an obvious solution to meet the demands of broadband, high power, THz sources. Gyro-devices are fast-wave sources and traditionally are based on a smooth-bore waveguide, rather than a slow-wave structure (SWS) that greatly limits the power handling capability of the THz sources. The gyro-backward wave oscillator (gyro-BWO) [5] and gyro-traveling wave amplifier (gyro-TWA) [6] are fast wave devices which can operate using higher order modes where the electrons are bunched in the azimuthal direction and do not rely on a SWS to longitudinally bunch the electrons in the beam.

The choice and design of the interaction region determines the THz source's power and maximum achievable tunability of the oscillator or bandwidth and gain of the amplifier. The helically corrugated interaction region (HCIR) [7] is one type of fast, beam-wave interaction region that has been used in gyro-amplifier experiments at X-band [8], [9], Ka-band [10], [11] and W-band [12]–[14]. Through coupling of two modes, one close to cutoff and the other far from cutoff, an eigenwave is formed that has preferential characteristics for wide band oscillation or broadband amplification. While experiments have been reported up to W-band, at higher frequencies the HCIR is technically challenging due to the need to maintain the Ohmic loss at a tolerable level and the difficulty of machining the part. However, it is possible to design and construct a 0.372 THz HCIR based on a 3-fold (3F) configuration [15]. State-of-the-art manufacturing facilities were required to build the 23.8 mm long 3F HCIR with an average diameter of 0.7 mm.

An 8-fold (8F) HCIR reduces the machining difficulty (but maintains the required accuracy) as it has a greatly enlarged geometry in comparison with the 3F HCIR, at an average diameter of 2.24 mm. Benefits of the larger diameter include: firstly, a more robust waveguide which allows longer sections to be manufactured removing misalignment issues, secondly it reduces electron beam optic sensitivity and allows for a higher power electron beam and hence higher millimetre wave output power to be generated. Furthermore, the ohmic losses are reduced which can be a limiting factor when operating at such high frequencies.

This paper also presents the design of the polarisation converter, 7-fold (7F) helically corrugated waveguide (HCW) mode converter and simulation of the higher order mode excitation of the 8F HCIR. The wave dispersion of the 8F HCIR was simulated and the maximum power handling capability calculated. The manufacture of the waveguide components and measurements of the wave properties of the 8F HCIR has validated the mode coupling in the HCIR.

II. Design

The HCIR and HCW have both an azimuthal and axial corrugation. It is described through the following relation, in cylindrical coordinates (r, θ, z).

$$r(\theta, z) = r_0 + r_1 \cos(m_B \theta + \frac{2\pi z}{d}) \quad (1)$$

This work was supported by the Engineering and Physical Sciences Research Council (EPSRC) U.K. under Research Grant EP/K029746/1 and EP/M008622/1 and Science and Technology Facilities Council (STFC) U.K. under Research Grant ST/T003227/1

C. R. Donaldson, L. Zhang, C. G. Whyte, and A. W. Cross are with the Scottish Universities Physics Alliance, Department of Physics, University of Strathclyde, Glasgow G4 0NG, U.K.

M. Harris, M. J. Beardsley, and P. G. Huggard are with the STFC Rutherford Appleton Laboratory, Didcot OX11 0QX, U.K.

W. He is with College of Electronics and Information Engineering, Shenzhen University, Shenzhen 518060, China.

Where, r_0 is the average radius, r_1 is the corrugation amplitude, d is the corrugation period and m_B is the fold number. The corrugated surface allows the resonant coupling of two normal waveguide modes (modes 1 and 2) provided they satisfy the synchronism conditions $k_1 \pm k_2 = 2\pi/d$ and $m_1 \pm m_2 = m_B$, where k is the axial wavenumber and m azimuthal indice of the modes. The twist of corrugations, and rotation of the waves, can be denoted as either left-handed (LH) or right-handed (RH). In a RH HCIR the traveling mode must rotate LH, against corrugations, otherwise a RH wave will see the HCIR as an equivalent smooth waveguide. The coupled mode can be either RH or LH depending on the sign of k_2.

In this paper, a HCIR was optimized with an eigenmode suitable for amplification at the desired centre frequency. It is achieved by coupling of the LH 1st spatial harmonic of the TE_{61} mode and the RH TE_{23} mode, with a fold number of $6+2=8$. The resonance conditions also allows the TE_{62} to couple with TE_{21} and TE_{22} modes, however coupling is weak and out of the interested frequency range [16]. A 4-fold $(6-2)$ HCIR can also couple the same set of modes (LH TE_{61} and LH TE_{23}), however simulation shows comparatively poorer bandwidth.

A mode converter is required as most sources output in the TE_{11} mode. Many mode converters exist based on desired input and output modes [17]–[19]. Another method is to use a 7F HCW mode converter to generate the TE_{61}. The profile of the HCW is similarly described by Eq. 1. The geometry of the 7F HCW mode converter is r_0 = 1.24 mm, r_1 = 0.07 mm, d = 2.33 mm with a total length of 11.65 mm and LH corrugations. The input RH TE_{11} mode converts to the LH TE_{61}, as shown in Fig. 2. If the same input mode rotates LH the lowest order mode that could be generated would be TE_{81}, however this is practically in cutoff and therefore the mode remains LH TE_{11} on exit from the HCW.

The mode converter was simulated using the CST Microwave Studio suite (CST-MS). A circularly polarised LH TE_{11} mode was excited at one port and the transmission to the other port calculated as shown in Fig. 1. At the centre frequency the transmission loss, in conversion to TE_{61}, was 0.55 dB. Away from the centre frequency the strength of the TE_{61} mode reduces and the resultant wave gains a higher content of the TE_{11} mode. An elliptical polarizer is used to convert the vector network analyzer (VNA) polarization from linear to circular. The geometry of the polariser consists of a circular waveguide (diameter 2.12 mm) that linearly tapers, over 10 mm length, to an elliptical shape (2.54 mm long axis by 2.12 mm short axis). The elliptical shape is maintained for a length of 17.30 mm, then it linearly tapers back to circular waveguide of 2.12 mm diameter. The polariser caused a small reduction in the conversion efficiency to the TE_{61} mode, 0.55 dB to 0.66 dB at 0.372 THz, shown in Fig. 1. The waveguide circuit, that includes the converters and 8F HCIR, is shown in Fig. 2.

The 8F HCIR has a desirable property of high power handling. Waveguide power handling is limited through two main factors, heating when operating at high average power, and electrical breakdown at high peak powers. The peak power

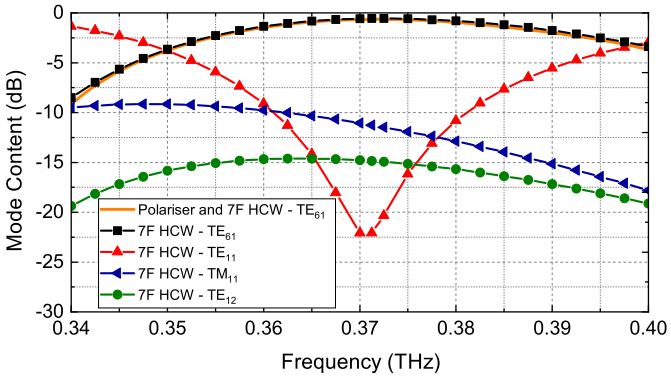

Fig. 1. Simulated transmission coefficient through the LH 7F HCW mode converter with an input RH TE_{11} mode.

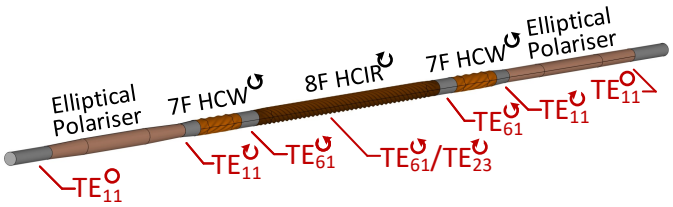

Fig. 2. The components and the waveguide modes in the THz system. The rotation of the waveguide modes and HCIR corrugation twist is shown.

will be considered here, while thermal analysis of HCWs is discussed in [20]. Such large interaction waveguides allow the propagation of relatively large diameter (and therefore high power) electron beams. Simultaneously the threshold for RF breakdown in the interaction region is raised. The combination of these two effects suggests that, if an electron beam of suitable parameters can be coupled to the desired operating mode, extremely high powers could be produced. The electric field strength of the eigenmode was calculated to be 0.96 MV/m with a 1 kW wave, at 0.372 THz, which equates to maintaining a maximum power of around 10 kW for continuous wave (CW) operation in air. This is around 14 times higher than the 3F HCIR at the same frequency. In pulsed operation a higher field can be tolerated, for example with a 10 ns pulse a field of 1 MV/cm [21], which equates to a maximum power of about 10 MW, was calculated.

III. Manufacture

The electroforming method was used as it allows solid singular parts to be manufactured which are vacuum tight as well as being able to meet the surface roughness and tolerance requirements. A negative of the waveguide component was machined into a sacrificial aluminium former. Copper was then electrolytically deposited onto the aluminium former in an acid bath. Sodium hydroxide is then used to remove the aluminium leaving the copper positive waveguide. The aluminium formers were made at the STFC Rutherford Appleton Laboratory. A Kern Micro computer numerical control (CNC) milling machine with an accuracy $\approx$1 μm was used in conjunction with high performance computer-aided manufacturing (CAM) software to generate complex toolpaths. The aluminium former

was first machined to a rod 0.1 mm larger in diameter than the outside diameter of the 7F HCW mode converter and the 8F HCIR. A 0.2 mm diameter ball end cutter was then used to form the helical groves. To dampen the vibrations and prevent sagging, the formers were held in a support block of Delrin. The mode converters with an elliptical polariser before each converter were manufactured on one aluminium rod, as shown in Fig. 3a. The 8F HCIR was made on an aluminium rod consisting of 36 periods of corrugations with a r_0 = 1.24 mm, r_1 = 0.09 mm, and d = 1.24 mm: Fig. 3b. All waveguides were electroformed to an external diameter of 8.00 mm.

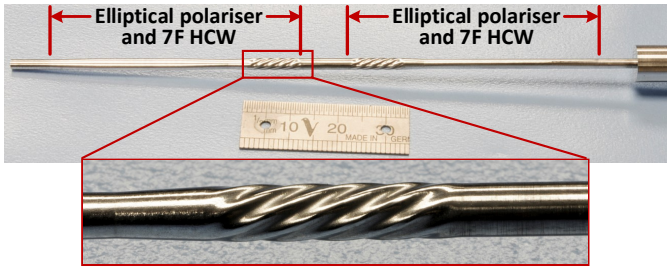

(a) The elliptical polariser and 7F HCW

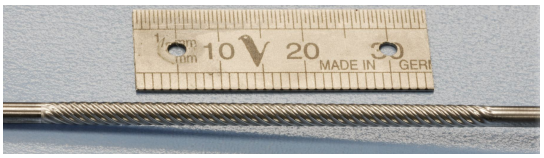

(b) The 8F HCIR

Fig. 3. Photographs of the aluminium formers.

IV. Measurement

A VNA was used to measure the wave properties of the 8F HCIR. The ports of the VNA have rectangular waveguides and hence rectangular to circular adapters were added to the transmit and receive millimeter-wave modules. The measurement was performed in two stages; the components shown in Fig. 2 were measured with, and then without, the 8F HCIR. The phase evolution was recorded in both sets of measurements and the phase change ($\Delta\theta$) only in the 8F HCIR was calculated. The two measurements are recorded with the polarisers in the two different configurations. The setting of the polariser determines whether the propagating wave rotates LH or RH into the mode converter. The exact measurement set-up was simulated using CST-MS with the phase change, and thus dispersion, of the different configurations, calculated. Coupled wave theory [16] was also used to calculate the eigenwave. The measured, simulated and calculated dispersions are shown in Fig. 4.

Outside the range 0.350 THz to 0.385 THz the mode converter cannot excite the correct mode efficiently and the performance is adversely affected. Inside these frequency limits agreement between modelling and measurement is excellent. The eigenmode calculated from coupled wave theory agrees very closely over the range 0.360 THz to 0.370 THz, where the polariser and mode converter performance is optimal. Outside this range we would not expect coupled wave theory

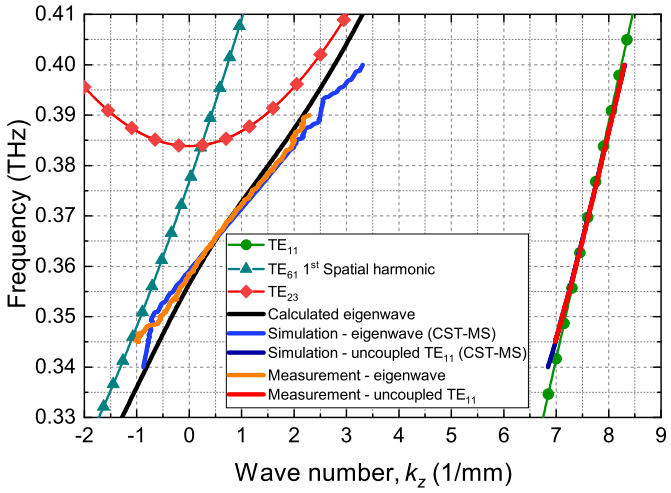

Fig. 4. Measured wave dispersion of an 8F HCIR as compared to analytical theory and CST-MS simulations.

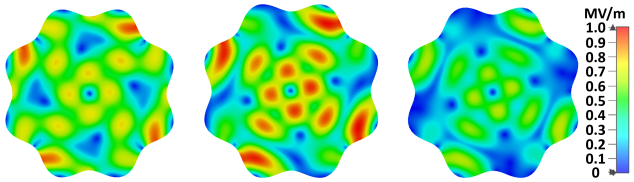

(a) 0.360 THz (b) 0.372 THz (c) 0.384 THz

Fig. 5. Simulated electric field at a cross section of the 8F HCIR with a 1 kW input wave at different input frequencies.

to accurately predict the result due to the change in mode mixture. This can be seen in Fig. 4 where the gradient of the coupled wave theory result diverges from the measured result at the frequency extremes. The simulated electric field in the 8F HCIR at different frequency points is shown in Fig. 5, indicating that the centre frequency of the eigenwave is 0.372 THz. When the polarisers are in the opposite direction the LH TE_{11} mode is input to the LH 7F HCW. The lowest order mode that could be generated would be the LH TE_{81} mode, which is practically in cutoff. In the RH 8F HCIR, the lowest order mode that could be generated by the LH TE_{11} mode is the RH TE_{71}. However, the coupling at the interested frequency range is weak and the output mode remains the LH TE_{11}. The measurement, and simulation, showed that the dispersion was almost a pure TE_{11} mode.

V. Conclusion

The design and measurement of an 0.372 THz 8F HCIR and mode converting 7F HCW have been presented in this paper. All components were manufactured using the method of electroforming onto precision machined mandrels. VNA measurements determined the waveguide dispersion of the 8F HCIR which agreed very well with the CST simulations and analytical calculations. The results reported in this paper demonstrate the feasibility of a high-fold HCIR operating with higher order modes opening up future applications in the THz frequency range.

REFERENCES

[1] G. L. Stephens, D. G. Vane, and R. J. B. et al., "The CloudSat mission and the A-Train," *Bull. Amer. Meteor. Soc.*, vol. 83, pp. 1773–1789, 2002, doi: 10.1175/BAMS-83-12-1771.

[2] R. I. Hunter, P. A. S. Cruickshank, D. R. Bolton, P. C. Riedi, and G. M. Smith, "High power pulsed dynamic nuclear polarisation at 94 GHz," *Phys. Chem. Chem. Phys.*, vol. 12, pp. 5752–5756, 2010.

[3] I. F. Akyildiz, J. M. Jornet, and C. Han, "Terahertz band: next frontier for wireless communications," *Physical Commun. J.*, vol. 12, pp. 16–32, 2014, doi: 10.1016/j.phycom.2014.01.006.

[4] M. Thumm, "State-of-the-art of high-power gyro-devices and free electron masers," *J. Infrared Milli. THz Waves.*, vol. 41, no. 1, pp. 1–140, 2020, doi: 10.1007/s10762-019-00631-y.

[5] C. T. Fan, T. H. Chang, K. F. Pao, and K. R. Chu, "Stable, high efficiency gyrotron backward-wave oscillator," *Phys. Plasmas*, vol. 14, no. 9, 093102, 2007, doi: 10.1063/1.2755964.

[6] K. R. Chu, "Overview of research on the gyrotron traveling-wave amplifier," *IEEE Trans. Plasma Sci.*, vol. 30, no. 3, pp. 903–908, 2002, doi: 10.1109/TPS.2002.801560.

[7] G. D. Denisov, V. L. Bratman, A. D. R. Phelps, and S. V. Samsonov, "Gyro-TWT with a helical operating waveguide: new possibilities to enhance efficiency and frequency bandwidth," *IEEE Trans. Plasma Sci.*, vol. 26, no. 3, pp. 508–518, 1998, doi: 10.1109/27.700785.

[8] G. D. Denisov, V. L. Bratman, A. W. Cross, W. He, A. D. R. Phelps, K. Ronald, S. V. Samsonov, and C. G. Whyte, "Gyrotron traveling wave amplifier with a helical interaction waveguide," *Phys. Rev. Lett.*, vol. 81, 5680, 1998, doi: 10.1103/PhysRevLett.81.5680.

[9] V. L. Bratman, A. W. Cross, G. G. Denisov, W. He, A. D. R. Phelps, K. Ronald, S. V. Samsonov, C. G. Whyte, and A. R. Young, "High-gain wide-band gyrotron traveling wave amplifier with a helically corrugated waveguide," *Phys. Rev. Lett.*, vol. 84, 2746, 2000, doi: 10.1103/PhysRevLett.84.2746.

[10] S. V. Samsonov, G. G. Denisov, I. G. Gachev, A. G. Eremeev, A. S. Fiks, V. V. Kholoptsev, G. I. Kalynov, V. N. Manuilov, S. V. Mishakin, and E. V. Sokolov, "CW Ka-band kilowatt-level helical-waveguide gyro-TWT," *IEEE Trans. Electron Dev.*, vol. 59, no. 8, pp. 2250–2255, 2012, doi: 10.1109/TED.2012.2196703.

[11] S. V. Samsonov, I. G. Gachev, G. G. Denisov, A. A. Bogdashov, S. V. Mishakin, A. S. Fiks, E. A. Soluyanova, E. M. Tai, Y. V. Dominyuk, B. A. Levitan, and V. N. Murzin, "Ka-band gyrotron traveling-wave tubes with the highest continuous-wave and average power," *IEEE Trans. Electron Dev.*, vol. 61, no. 12, pp. 4264–4267, 2014, doi: 10.1109/TED.2014.2364623.

[12] W. He, C. R. Donaldson, L. Zhang, K. Ronald, A. D. R. Phelps, and A. W. Cross, "Broadband amplification of low-terahertz signals using axis-encircling electrons in a helically corrugated interaction region," *Phys. Rev. Lett.*, vol. 119, 184801, 2017, doi: 10.1103/PhysRevLett.119.184801.

[13] L. Zhang, C. R. Donaldson, P. Cain, A. W. Cross, and W. He, "Amplification of frequency-swept signals in a W-band gyrotron traveling wave amplifier," *IEEE Electron Dev. Lett.*, vol. 39, no. 7, pp. 1077–1080, 2018, doi: 10.1109/LED.2018.2836868.

[14] S. V. Samsonov, G. G. Denisov, I. G. Gachev, and A. A. Bogdashov, "CW operation of a W-band high-gain helical-waveguide gyrotron traveling-wave tube," *IEEE Electron Dev. Lett.*, vol. 41, no. 5, pp. 773–776, 2020, doi: 10.1109/LED.2020.2980572.

[15] C. R. Donaldson, L. Zhang, M. Beardsley, M. Harris, P. G. Hugard, and W. He, "CNC machined helically corrugated interaction region for a THz gyrotron traveling wave amplifier," *IEEE Trans. THz Sci. Techn.*, vol. 8, no. 1, pp. 85–89, 2017, doi: 10.1109/TTHZ.2017.2778944.

[16] L. Zhang, W. He, K. Ronald, A. D. R. Phelps, C. G. Whyte, C. W. Robertson, A. Y. Young, C. R. Donaldson, and A. W. Cross, "Multi-mode coupling wave theory for helically corrugated waveguide," *IEEE Trans. Microw. Theory Techn.*, vol. 60, no. 1, pp. 1–7, 2012, doi: 10.1109/TMTT.2011.2170848.

[17] Y. Wang, "Wideband circular TE_{21} and TE_{01} mode converters with same exciting topologies," *IEEE Trans. Electron Devices*, vol. 63, no. 10, pp. 4088–4095, 2016, doi: 10.1109/TED.2016.2596785.

[18] C. Schulz, C. Baer, T. Musch, I. Rolfes, and B. Will, "Investigation of a circular TE_{11}-TE_{01}-mode converter in stepped waveguide technique," *Int. J. Microw. Wireless Technol.*, vol. 7, no. 3-4, pp. 229–237, 2015m doi: 10.1017/S1759078715000203.

[19] G. G. Denisov, G. I. Kalynova, and D. I. Sobolev, "Method for synthesis of waveguide mode converters," *Radiophys. Quantum Electron.*, vol. 47, no. 8, pp. 615–620, 2004, doi: 10.1023/B:RAQE.0000049559.74097.86.

[20] S. V. Mishakin and S. V. Samsonov, "An approach to thermal analysis of helically corrugated waveguide elements of vacuum electron devices," *IEEE Trans. Micro. Theory Techn.*, vol. 66, no. 12, pp. 5206–5211, 2018, doi: 10.1109/TMTT.2018.2873362.

[21] A. V. Gunin, A. I. Klimov, S. D. Korovin, I. K. Kurkan, I. V. Pegel, S. D. Polevin, A. M. Roitman, V. V. Rostov, A. S. Stepchenko, , and E. M. Totmeninov, "Relativistic X-band BWO with 3-GW output power," *IEEE Trans. Plasma Sci.*, vol. 26, no. 3, pp. 326–331, 1998, doi: 10.1109/27.700761.